International Journal of Quantum Information
Vol. 10, No. 6 (2012) 1250063 (16 pages)

DOI: 10.1142/S0219749912500633

TYPICAL BEHAVIOR OF THE GLOBAL ENTANGLEMENT OF AN OPEN MULTIQUBIT SYSTEM IN A NON-MARKOVIAN REGIMEN

A. P. MAJTEY

Instituto Carlos I de Física Teórica y Computacional, and Departamento de Física Atómica Molecular y Nuclear, Universidad de Granada, Granada, E-18071, Spain
anamajtey@gmail.com

A. R. PLASTINO

Instituto Carlos I de Física Teórica y Computacional, and Departamento de Física Atómica Molecular y Nuclear, Universidad de Granada, Granada, E-18071, Spain

Universidad Nacional de La Plata, CREG-UNLP, C. C. 727, 1900 La Plata, Argentina

Received 7 March 2012
Revised 20 July 2012
Accepted 17 August 2012
Published 18 October 2012

We investigate the decay of the global entanglement, due to decoherence, of multiqubit systems interacting with a reservoir in a non-Markovian regime. We assume that during the decoherence process each qubit of the system interacts with its own, independent environment. Most previous works on this problem focused on particular initial states or families of initial states amenable of analytical treatment. Here we determine numerically the typical, average behavior of the system corresponding to random initial pure states uniformly distributed (in the whole Hilbert space of n-qubit pure states) according to the Haar measure. We study systems consisting of 3, 4, 5, and 6 qubits. In each case we consider also the entanglement dynamics corresponding to important particular initial states, such as the GHZ states or multiqubit states maximizing the global entanglement, and determine in which cases any of these states is representative of the average behavior associated with general initial states.

Keywords: Decoherence; non-Markovian dynamics; entanglement.

PACS Number(s): 03.65.Yz, 03.67.Mn, 03.67.-a

1. Introduction

Decoherence is a quantum phenomenon that plays an important role in connection both with the foundations of quantum physics and with its technological applications.[1–3] Decoherence is inextricably linked to another basic ingredient of the

quantum world: Quantum entanglement.[4–7] Indeed, the diverse effects associated with the phenomenon of decoherence are due to the development of entanglement between the system under consideration and its environment. This entanglement, arising from the interaction between an imperfectly isolated system and its surroundings, leads to the gradual disappearance of various quantum features exhibited by the system. These effects are at the core of the nowadays orthodox, decoherence-based explanation of the quantum-to-classical transition.[1]

One of the most important consequences of decoherence is that the (internal) entanglement between the different parts of a composite system undergoing decoherence tends to decay. This manifestation of decoherence constitutes one of the main hurdles that has to be overcome for the implementation of quantum technologies that require entangled states as a resource.[2] The decay of entanglement under decoherence has been the focus of an intense research activity in recent years.[8–20] A particularly interesting feature of this process, first pointed out by Zyczkowski and the Horodeckis in a pioneering effort almost ten years ago,[21] is that sometimes entanglement vanishes completely in a finite time. This remarkable phenomenon, known as entanglement sudden death (ESD), has been the subject of several theoretical and experimental studies.[22–37]

Studies of ESD in Markovian scenarios suggested that, once entanglement has vanished due to decoherence, this valuable resource is irremediably lost. However, the decoherence process in non-Markovian regimes sometimes gives rise to an interesting new effect: Entanglement sudden revival. The sudden revival of entanglement after a finite time interval with zero entanglement following an ESD event has been recently investigated in Refs. 27 and 28. These works considered a system consisting of two independent qubits interacting with an environment at zero temperature in a non-Markovian regime. The entanglement dynamics of open multiqubit systems in non-Markovian regimes has also been considered in various recent works.[29,30,32] In particular, multiqubit systems evolving from initial GHZ or W states have been studied in detail in Refs. 29 and 30. On the other hand, the average, typical entanglement-related features corresponding to some families of initial states of 2-qubit, 3-qubit, and 4-qubit systems have been investigated in Ref. 32.

The phenomenon of entanglement sudden revival allowed by non-Markovian regimes deserves detailed scrutiny: It is of clear interest from the fundamental point of view and may also have technological implications. The aim of the present contribution is to explore (statistically) the typical behavior of the entanglement exhibited by multipartite systems interacting with the above mentioned environment. In contrast to previous studies of entanglement evolution in non-Markovian regimes, that focused on particular states or particular families of states, we will explore the average, typical entanglement dynamics associated with random, general initial pure states uniformly distributed according to the Haar measure. We are also going to consider the average behavior corresponding to mixed initial states consisting of a mixture of a (random) pure state and the totally mixed state.

The article is organized as follows. A brief description of the system studied here is provided in Sec. 2. Our main findings concerning the typical entanglement evolution of n-qubit systems are detailed in Sec. 3. Finally, some conclusions are drawn in Sec. 4.

2. System-Reservoir Model

We are going to explore the typical, average features characterizing the entanglement dynamics of an open system consisting of n independent qubits evolving in a non-Markovian regime. These n-qubits evolve from an initial entangled state generated through some previous, unspecified, interacting process. Each of the above mentioned qubits experiences the same decoherence process, which is due to the interaction of the qubit with its own environment. The evolution of the density matrix ρ_i of the i-qubit is given by a completely positive trace-preserving map that admits a Kraus representation of the form,

$$\rho_i(0) \to \rho_i(t) = \sum_{j=1}^{M} E_{ji}\rho_i(0)E_{ji}^{\dagger}, \tag{1}$$

where E_j: $j = 1, \ldots, M$ constitute an appropriate set of Kraus operators yielding a complete description of the single qubit's dynamics. The evolution of the total density matrix ρ corresponding to the entire n-qubit system can also be expressed in terms of the above Kraus operators,

$$\rho(0) \to \rho(t) = \sum_{i\cdots j} E_{i1} \otimes \cdots \otimes E_{jn}\rho(0)[E_{i1} \otimes \cdots \otimes E_{jn}]^{\dagger}. \tag{2}$$

We are going to assume that the dynamics of each qubit of the system is determined by a "qubit + reservoir" interaction given by the paradigmatic Hamiltonian,[27]

$$H = \omega_0\sigma_+\sigma_- + \sum_k \omega_k b_k^{\dagger}b_k + \sum_k g_k(\sigma_+ b_k + \sigma_- b_k^{\dagger}), \tag{3}$$

where ω_0 is the transition frequency of an atomic two-level system (qubit), σ_+, σ_- are the atomic raising and lowering operators, $b_k^{\dagger}$, b_k are the creation and annihilation operators of the reservoir's (electromagnetic) k-mode, and ω_k, g_k denote the corresponding frequency and coupling constant (with the qubit). A possible physical realization of a system governed by the Hamiltonian (3) is given by a two-level atom interacting with a reservoir consisting of the electromagnetic modes of a high-Q cavity. Following[27] we adopt for the reservoir an effective spectral density of the form

$$J(\omega) = \frac{1}{2\pi}\frac{\gamma_0\lambda^2}{(\omega_0 - \omega)^2 + \lambda^2}. \tag{4}$$

The parameter λ, defining the spectral width of the coupling, is then connected to the reservoir correlation time τ_b trough $\tau_b \sim \lambda^{-1}$. On the other hand, the parameter

γ_0 is associated with the system's relaxation time τ_R according to the relation $\tau_R \sim \gamma_0^{-1}$ (see Ref. 27 for details). Non-Markovian dynamics is obtained in the strong-coupling regime given by the inequality $\gamma_0 > \lambda/2$. The time dependent density matrix describing the behavior of a single qubit has the form

$$\rho(t) = (\rho_{00}(0) + \rho_{11}(0)(1 - p_t))|0\rangle\langle 0| + \rho_{01}(0)\sqrt{p_t}|0\rangle\langle 1| + \rho_{10}(0)\sqrt{p_t}|1\rangle\langle 0| + \rho_{11}(0)p_t|1\rangle\langle 1|, \tag{5}$$

where the $\rho_{ij}(0)$ denote the elements of the initial density matrix, and p_t is given by

$$p_t = \mathrm{e}^{-\lambda t}\left[\cos\left(\frac{dt}{2}\right) + \frac{\lambda}{d}\sin\left(\frac{dt}{2}\right)\right]^2, \tag{6}$$

where $d = \sqrt{2\gamma_0\lambda - \lambda^2}$.[27] In the present work we are going to focus on the non-Markovian regime, setting $\lambda = 0.01\gamma_0$ in all our computations.

It can be verified, after some algebra, that the evolution of the single-qubit reduced density matrix elements given by (5) admits a representation of the form (1) involving the following pair of Kraus operators,

$$E_0 = |0\rangle\langle 0| + \sqrt{p_t}|1\rangle\langle 1|,$$
$$E_1 = \sqrt{1 - p_t}|0\rangle\langle 1|. \tag{7}$$

By recourse to Eq. (2) the alluded Kraus representation of the single-qubit dynamics can be used to obtain the full dynamics characterizing the whole n-qubit system.

3. Typical Entanglement Dynamics for n-Qubits

3.1. *Preliminaries*

We are going to study the average entanglement dynamics associated with random initial multiqubit pure states. These initial states are of the form

$$|\Psi\rangle = U^{(n)}|\Psi_0\rangle, \tag{8}$$

where $|\Psi_0\rangle$ is a fixed n-qubit state, and $U^{(n)}$ is a random unitary transformation acting on the multiqubit system. The unitary transformations $U^{(n)}$ are generated according to the uniform distribution determined by the Haar measure (see Ref. 38 and references therein). To evaluate the average properties of the entanglement dynamics of the n-qubit system we determine the entanglement evolutions corresponding to many initial states generated according to the procedure explained, and compute the concomitant mean entanglement evolution.

We also investigate the entanglement dynamics of random mixed states of the form,

$$\rho_{\text{mixed}} = x|\Psi\rangle\langle\Psi| + \frac{(1-x)}{2^n}\mathbb{I}, \tag{9}$$

with $0 \leq x \leq 1$. Here x is the purity of the multipartite state, $\mathbb{I}$ is the $n \times n$ identity operator, and $|\Psi\rangle$ is a random pure state generated following the same procedure as the one used to generate random initial pure states.

To quantify the entanglement of a multipartite state one can deal with measures defined as the average of bipartite entanglement measures over all the possible bi-partitions of the system. This is usually known as global entanglement and a considerable amount of research has recently been devoted to its study (see Refs. 39, 40 and references therein). The global entanglement E can be expressed as follow,

$$E = \frac{1}{[n/2]} \sum_{m=1}^{[n/2]} E^{(m)}, \tag{10}$$

$$E^{(m)} = \frac{1}{K^{(m)}_{\text{bipart}}} \sum_{\text{bipart}} E(\text{bipart.}). \tag{11}$$

In Eqs. (10) and (11) the possible bi-partitions of the n-qubit system are grouped in families corresponding to partitions into two sub-systems with given numbers of constituting qubits. $E^{(m)}$ denotes the average entanglement associated with the particular family comprising the $K^{(m)}_{\text{bipart}}$ nonequivalent bi-partitions of the system into two subsystems having, respectively, m and $n-m$ qubits. The sum appearing in Eq. (11) has, therefore, $K^{(m)}_{\text{bipart}}$ terms. $E(\text{bipart.})$ stands for the entanglement associated with one single bi-partition of the n-qubit system.

The above procedure for evaluating a global entanglement measure on the basis of bi-partitions can be implemented in a variety of ways, depending on which measure $E(\text{bipart.})$ one uses to evaluate the entanglement of the individual bi-partitions. When dealing with mixed states the negativity constitutes the most important and most widely used, practical bipartite entanglement measure. The negativity $N(\text{bipart.})$ corresponding a given bipartition of the system into two subsystems, one with m qubits and the other one with $n-m$ qubits, with $m \leq n-m$, is given (up to a normalization multiplicative factor) by the sum of the negative eigenvalues α_i of the partial transpose matrix associated with this bipartition,

$$N(\text{bipart.}) = \frac{2}{2^m - 1} \sum_i |\alpha_i|. \tag{12}$$

In this work we also consider an indicator of entanglement E_{MB} proposed by Mintert and Buchleitner[41] which is given by

$$E_{\text{MB}}[\rho] = 2Tr[\rho^2] - Tr[\rho_1^2] - Tr[\rho_2^2], \tag{13}$$

with ρ_1 and ρ_2 the reduced density matrices of the associated subsystems. The entanglement indicator E_{MB} constitutes a lower bound of the squared concurrence, which for mixed states ρ is defined as[42]

$$C[\rho] = \inf \sum_i p_i C(\Psi_i), \tag{14}$$

where $\{p_i, \Psi_i\}$ $(\sum_i p_i = 1)$ are all the possible decompositions of ρ into mixtures of pure states $|\Psi_i\rangle$, and C is the concurrence of a pure state of a bipartite system,

$$C(\Psi) = \sqrt{2[1 - Tr(\rho_r^2)]}, \tag{15}$$

with ρ_r the marginal density matrix corresponding to either subsystem.

3.2. *Pure states*

In this section we determine numerically the decay of the average entanglement of a multiqubit system when considering general, random initial pure states uniformly generated according to the Haar measure. All exhibited curves are obtained generating (and averaging over) 10^4 random pure states. See the Appendix A for technical details on this choice of the sample size. The main results obtained by us are summarized in Figs. 1–4. In Figs. 1(a)–1(d) we plot (for systems of 3, 4, 5, and 6 qubits, respectively) the average entanglement $\langle N \rangle$ and the dispersion $\Delta N = \sqrt{\langle N^2 \rangle - \langle N \rangle^2}$ as a function of the dimensionless quantity $\gamma_0 t$. The dispersion ΔN gives an estimation of the width of the entanglement distribution associated with initial random states. In all cases it is seen that ΔN is relatively small compared with $\langle N \rangle$, which means that this last quantity is representative of the typical entanglement dynamics exhibited by the multiqubit system. In Fig. 1 we also depict the curves corresponding to the entanglement decay of some important particular states, such as the n-qubit GHZ state (which is the maximally entangled state in the 3 qubit case) and the maximally entangled states for 4, 5, and 6 qubit systems (the corresponding curves in Figs. 1(c) and 1(d) are identified with the label "robust", for reasons explained below). For systems of 4 qubits we compute the entanglement evolution of the state HS, which was introduced by Higuchi and Sudbery[43] (see also Ref. 40). This state has been conjectured to maximize the entanglement of 4-qubit states[43] and, even if a proof of this conjecture is still lacking, various analytical and numerical evidences supporting it have been reported in the literature.[39,40,43] In the cases of five and 6-qubit systems we plot the entanglement decay for the maximally entanglement states $|\Phi_{5qb}^{\mathrm{ME}}\rangle$[39] and $|\Phi_{6qb}^{\mathrm{ME}}\rangle$.[40] The HS 4-qubit state and the $|\Phi_{6qb}^{\mathrm{ME}}\rangle$ 6-qubit states are specially relevant in connection with the process of decoherence because they also constitute robust states under decoherence. In a previous work[19] we have numerically determined these robust states for systems of 4, 5, and 6 qubits under different (Markovian) decoherence processes. By a "robust state" we mean an

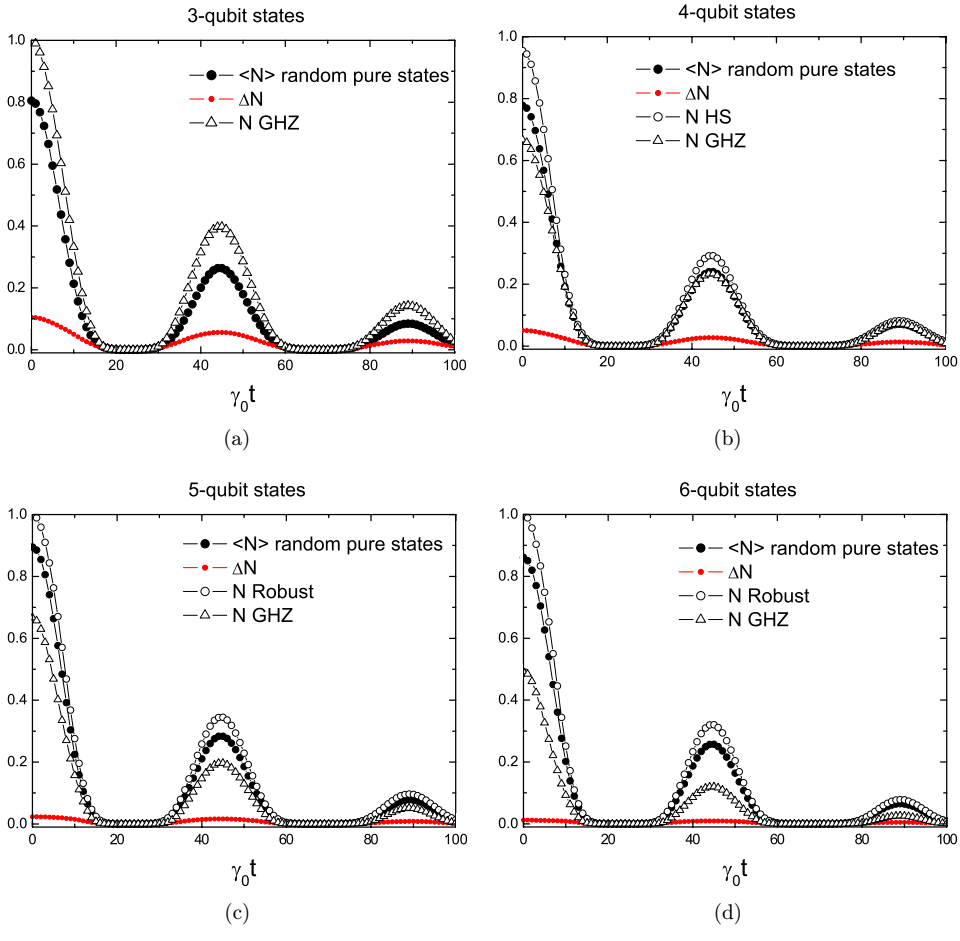

Fig. 1. Entanglement evolution of the 3, 4, 5, and 6 qubits random (pure) states under decoherence. All depicted quantities are dimensionless.

initial state evolving under decoherence to states that are, at any given time, more entangled than those generated by alternative initial states. The 5-qubit state $|\Phi_{5qb}^{\mathrm{ME}}\rangle$ does not coincide with the robust state reported in Ref. 19, but in the case of the dynamics studied in the present work, our numerical results indicate that both states lead to the same (or very close) average entanglement evolution.

A particularly interesting aspect of Figs. 1(a)−1(d) is the status of the state GHZ with respect to the typical behavior of the entanglement dynamics of the multiqubit system. In the case of 3-qubit systems the time dependent average entanglement is appreciably below the entanglement of states that evolved from the GHZ one, particularly at those times when the system's entanglement reaches its maximum values. The situation is different in the case of 4 qubits, where we found that the entanglement dynamics associated with a GHZ initial state is quite representative of the

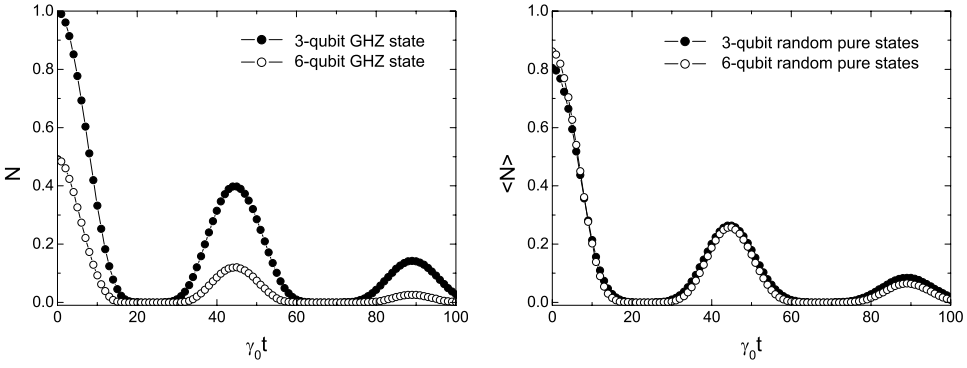

(a) (b)

Fig. 2. Entanglement evolution of the 3-qubit and 6-qubit representative states under decoherence: (a) GHZ states of 3 and 6 qubits; (b) Random pure states of 3 and 6 qubits. All depicted quantities are dimensionless.

typical, average dynamics associated with random initial states. On the other hand, for systems of 5 and 6 qubits the entanglement evolution associated with the GHZ state does not reflect the average behavior, which is more closely represented by the entanglement dynamics exhibited by states respectively evolving from the previously mentioned $|\Phi_{5qb}^{\mathrm{ME}}\rangle$ and $|\Phi_{6qb}^{\mathrm{ME}}\rangle$ states.

Evidence has been previously reported suggesting that in some situations the robustness of entanglement may increase with the number of qubits in the system.[8] However, recent investigations[12] indicate that, even when entanglement takes a long time to disappear, it rapidly adopts values too small to be of any practical relevance for technological applications. It is interesting to explore the dependence of the entanglement robustness on the number of qubits within the context of the non-Markovian evolution studied in the present work. Some results pertaining to this issue are summarized in Figs. 2 and 3. In Fig. 2(a) we compare the entanglement evolution yielded by initial GHZ states of systems of three and 6-qubits. It transpires from this figure that the finite time intervals of zero entanglement are longer in the case of 6 qubits than in the case of 3 qubits. This suggests that the lengths of these intervals tend to increase with the number of qubits, consistently with other results for particular states recently reported in Ref. 32. This trend, however, is not observed when we evaluate the average entanglement evolution corresponding to random initial pure states, as can be appreciated in Fig. 2(b). Furthermore, the average entanglement evolutions corresponding to random initial pure states of systems consisting of 3, 4, 5, and 6 qubits are depicted in Fig. 3, showing an almost universal pattern. The average entanglement of random initial pure states thus seems to be less fragile than the entanglement corresponding to the GHZ state. It is interesting to compare these findings with those reported in a recent study by Aolita *et al.*[15] These authors investigated the decay of the entanglement under various decoherence channels of the GHZ state. Aolita *et al.* determined an upper bound for the

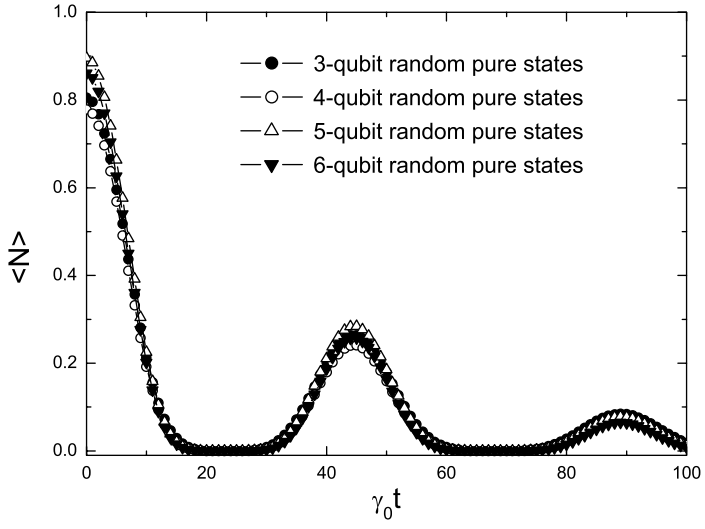

Fig. 3. Average entanglement evolution under decoherence corresponding to random initial pure states of systems of 3, 4, 5, and 6 qubits. All depicted quantities are dimensionless.

entanglement of states evolved (under the alluded decoherence channels) from initial GHZ states. They found, however, that the average entanglement of states evolved from random initial pure states does not comply with this bound, suggesting that the exponentially increasing fragility of the GHZ entanglement with the number of qubits of the system is not a generic feature of typical pure states. Our present results constitute further evidence also pointing towards the conclusion that the exponential (in terms of system's size) fragility of the GHZ state may be a peculiarity of this state not shared by generic ones. On the contrary, general pure states, on average, seem to exhibit more robust entanglement than the GHZ state. Another finding that is relevant in connection with this problem was reported by Hein *et al.*,[11] where it was shown that the entanglement decay under decoherence corresponding to certain graph states states is very different from the one characterizing the GHZ states. The entanglement decay associated with graph states with a constant degree (not dependent on the number of qubits) does not become more acute as the size of the system increases. Results indicating that the entanglement fragility of the GHZ states is not a generic feature of multiqubit states were also presented by Carvalho *et al.*[9] who showed that the rates of (exponential) decay of entanglement of the W sates are independent of the number of qubits of the system in the cases of coupling to a zero temperature bath and of dephasing. On the contrary, under these environmental influences the entanglement decay rate grows linearly with the number of qubits for the GHZ state.

Let us denote by $\langle N^{(m)} \rangle$ the average negativity corresponding to all the partitions of the system into two subsystems having, respectively, m and $n - m$ qubits. In Fig. 4 we compare for 4 and 5 qubit systems the evolution of the entanglement of the most

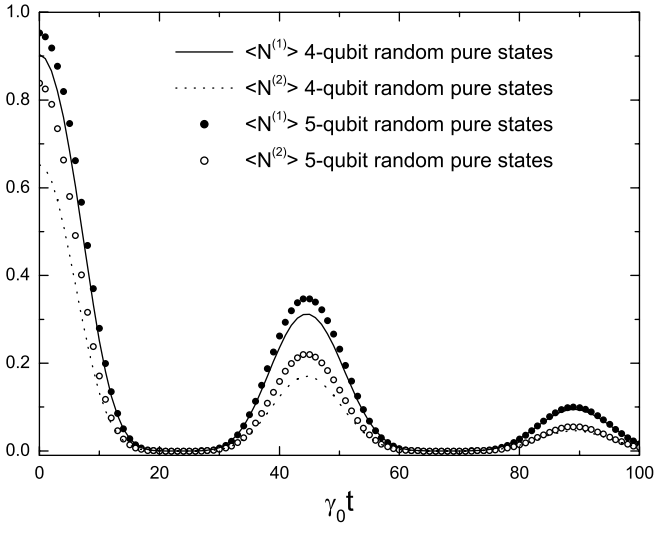

Fig. 4. Entanglement evolution of the random 4 (lines) and 5 (dots) qubit systems under decoherence for the most unbalanced (solid line, full dots) and most balanced (dotted line, empty dots) possible bipartitions of the systems. All depicted quantities are dimensionless.

balanced bipartitions $\langle N^{(2)}\rangle$ and the most unbalanced ones $\langle N^{(1)}\rangle$. We can see that the behavior exhibited by the negativities corresponding to these special bipartitions is very similar to that of the global negativity $\langle N\rangle$.

The dynamical evolution of the average $\langle E_{\rm MB}\rangle$ is compared with that of the negativity in Fig. 5, for 4 and 5 random qubit systems. In both cases the quantity $E_{\rm MB}$ is able to detect entanglement only during the first period of entanglement decrease, but it does not detect the subsequent entanglement revivals. This is consistent with the fact that the quality of the entanglement indicator $E_{\rm MB}$ tends to

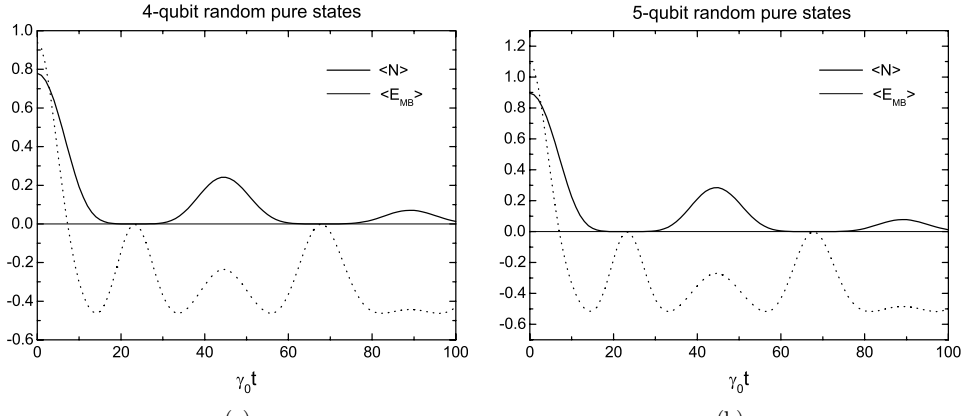

Fig. 5. The negativity and the $E_{\rm MB}$ entanglement indicator as a function of $\gamma_0 t$ for random 4 (a) and 5 (b) initially pure qubit systems. All depicted quantities are dimensionless.

deteriorate as one considers states of increasing mixedness,[44] and the multiqubit systems under consideration here have a considerable degree of mixedness during the entanglement revival events.

It is known that the entanglement exhibited by composite quantum systems tends to decrease as we consider states with increasing degree of mixedness. It is interesting to notice that the average entanglement evolution of the system under consideration in the present work does not follow this general tendency. The average time evolution of both the negativity and the degree of mixedness (as measured by the linear entropy S_L of the time dependent state) corresponding to random initial pure states of 6 qubits are depicted in Fig. 6. We can see that, except for the initial entanglement decrease, the moments of high entanglement tend to coincide with moments of high mixedness. This point was recently highlighted in Ref. 35, in connection with the evolution of systems of 2 qubits, and is also consistent with previous results advanced in Ref. 32. Before discussing in more detail this aspect of the evolution of the multiqubit systems discussed here it is worth mentioning that this behavior is atypical but should not be regarded as paradoxical. Even if, as a general tendency, entanglement tends to decrease when the degree of mixedeness increases, there is no strict correlation between these two quantities. It is indeed possible to find pairs of states such that the state with higher mixedness is also the more entangled one. In spite of this, it is still interesting that the system's evolution considered here consists (during certain time intervals) of states showing this somewhat atypical characteristic.

To understand better this peculiarity let us first notice that the system's entanglement vanishes at those times when the parameter p_t becomes equal to zero, $p_t = 0$. At these times the mixedness of the multiqubit system also vanishes, because its state is given by $\rho_s = (|0\rangle\langle 0|)^{\otimes n}$, which is pure and separable. When starting from an initial entangled pure state $\rho_i = |\Psi\rangle\langle\Psi|$, the evolution of the system's mixedness can be construed as arising from two opposite tendencies. First, due to the interaction with

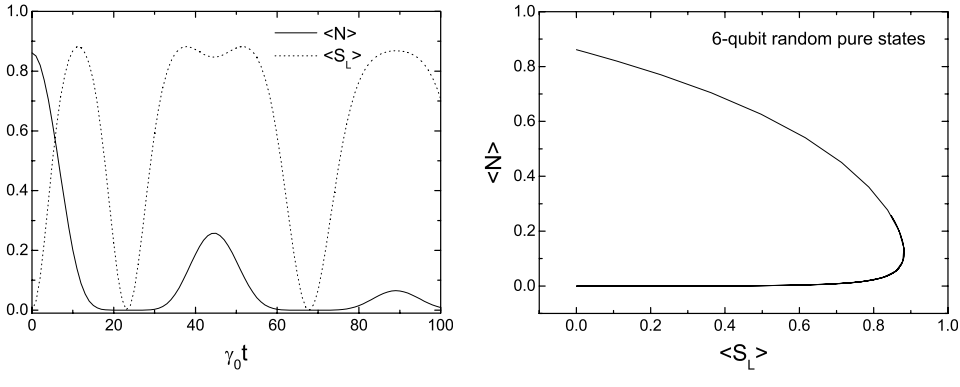

Fig. 6. Average time evolution of the global entanglement and the linear entropy corresponding to random initial 6-qubit pure states (a) and the mean global entanglement versus the mean linear entropy associated with those states (b). All depicted quantities are dimensionless.

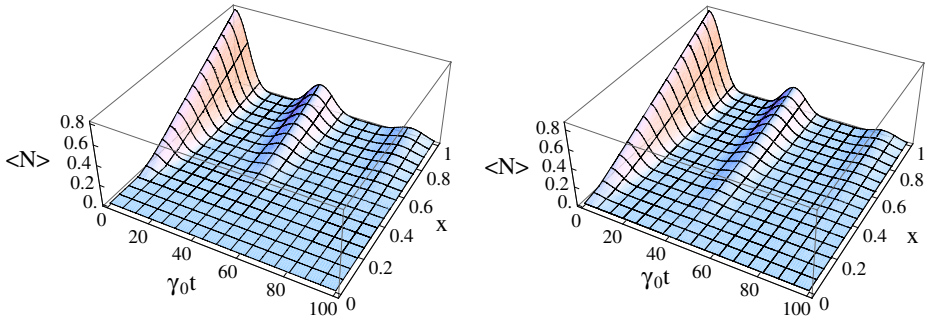

Fig. 7. Time evolution of $\langle N \rangle$ for random initial n-qubit mixed states of the form (9) as a function of $\gamma_0 t$ and x, for $n = 3$ (left) and $n = 6$ (right). All depicted quantities are dimensionless.

its surroundings, some entanglement is developed between the system and the environment and the system's mixedness tends to increase. On the other hand, as the evolution proceeds, the system eventually begins to approach the pure state ρ_s, and its mixedness, after having achieved a maximum value, starts to decrease again. Consequently, the resulting evolution comprises an initial phase of monotonous increase in the degree of mixedness followed by a period of decreasing mixedness during which its value goes back to zero. On the other hand, during this whole time interval

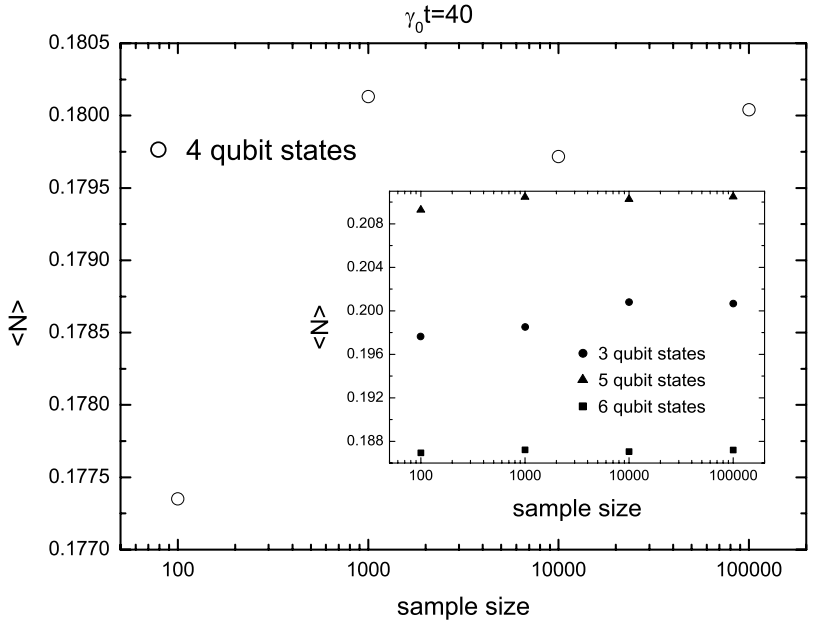

Fig. 8. $\langle N \rangle$ as a function of the sample size for 4 qubit random states. Inset: $\langle N \rangle$ as a function of the sample size for 3 (circle), 5 (triangle), and 6 (square) qubit random states. All depicted quantities are dimensionless.

before p_t achieves its first zero, the system's entanglement decreases monotonously, finally vanishing when $p_t = 0$. Notice that during the second half of this period, during which the system is evolving towards ρ_s, the system's entanglement and mixedness both decrease together and finally vanish when $p_t = 0$. After this, when p_t starts increasing again during the first entanglement revival, the system's entanglement and degree of mixedness grow together, reaching their respective maximum values approximately at the same time and then decreasing together as the system evolves back to the state ρ_s.

3.3. *Mixed initial states*

Here we consider the entanglement decay of states of the form (9), consisting of a statistical mixture of a pure state $|\Psi\rangle$ and the totally mixed state. Our results are given in Fig. 7, where the average negativity $\langle N\rangle$ is plotted against $\gamma_0 t$ and the parameter x for systems of 3 and 6 qubits. We see that the general patterns associated with these two cases are similar except for the fact that the average negativity of systems having 6 qubits decreases more slowly with x than the average negativity corresponding to systems of 3 qubits.

4. Conclusions

When considering the average behavior of generic initial pure states of multiqubit systems for $n = 3$, 4, 5, and 6 qubits one obtains in each case a very similar, almost universal pattern of entanglement evolution. This is an interesting result, specially in connection with some previous studies suggesting that entanglement becomes more robust as the size of the system increases. It is clear that the system under study here does not follow that trend. Nor does the average entanglement become appreciably more fragile as the number of qubits increases, at least within the range of n-values considered by us.

In the cases of systems having 5 and 6 qubits, the robust states studied in Ref. 19 exhibit, under the dynamics considered in the present work, a behavior that is quite close to the average behavior corresponding to generic initial pure states. In this sense, the entanglement dynamics of the alluded robust states is representative of the typical dynamics of initial pure states. On the contrary, the average entanglement dynamics of 5 and 6 qubits departs from the one exhibited by the corresponding GHZ states, whose entanglement appears to be more fragile than the entanglement of typical, average, pure states. These findings are consistent with other recent results in the literature, also indicating that the entanglement fragility of GHZ states under various decoherence channels is not a generic feature of typical multiqubit pure states.

Systems of 4 qubits show some peculiarities. In the case of these systems the average entanglement evolution of random initial pure states is quite similar to the entanglement evolution corresponding to an initial GHZ state.

The observed universal features exhibited by the average entanglement dynamics associated with random initial pure states of n-qubits is plausibly related to the fact that each qubits is interacting with its "own" independent heat bath. This fact implies that the typical behaviors of systems with different (total) numbers n_1 and n_2 of qubits, even though they are not identical, share some important features: The evolution rules for the local states of blocks of L qubits (with $L \leq \min(n_1, n_2)$) are the same in both cases. For instance, the evolution equation for single qubits is always given by Eq. (1).

The fact that the GHZ states deviate from the typical behavior, having entanglement features that are more fragile than those of typical initial states, is consistent with other known manifestations of the "fragility" of the quantum correlations exhibited by these states. For instance, it is well-known that if we trace over one of the qubits of a system initially described by a GHZ state, the remaining $n-1$ qubits are left in a mixed nonentangled state. Also, if we measure the state of one of the qubits, the remaining qubits are left in a nonentangled state. These properties are in contrast with the ones exhibited by other multiqubit entangled states, such as the W states, where some entanglement survives after measuring the state of one of the parts of the system. As a final remark concerning GHZ states, it is worth mentioning that for systems having five or more qubits the difference between the entanglement of the maximally entangled states (according to the partitions-based measures considered here) and the GHZ states is much larger than in the case of systems of 4 qubits. This may be related to the fact that the behavior of GHZ states deviate more from the average behavior in the case of systems with five or more qubits, than in the case of systems with 4 qubits.

The main results presented in this work have been obtained using entanglement measures based upon the negativities associated with the different possible bi-partitions of the multiqubit system. We focused mostly on the behavior exhibited by the global mean value corresponding to all those bi-partitions. However, the entanglement dynamics corresponding to particular bi-partitions was also considered, and the results obtained are similar to those corresponding to the global average. The negativity, even though it provides one particular way of quantitatively characterizing the amount of entanglement in composite quantum systems, it constitutes one of the most widely used *practical* tools for studying the entanglement of mixed states. It would be interesting to explore other ways of characterizing the evolution of the entanglement (or other manifestations of quantum mechanical correlations) of the system considered here. Any further developments along these lines will be very wellcome.

Acknowledgments

This work was partially supported by the Projects FQM-2445 and FQM-207 of the Junta de Andalucia, and the grant FIS2011-24540 of the Ministerio de Innovación y Ciencia (Spain). A.P.M. acknowledges support by GENIL trhough YTR-GENIL Program.

Appendix A. Details of the Numerical Calculations

In this appendix we provide some technical details on the numerical Monte Carlo procedure employed to compute the average properties corresponding to general initial pure states of the multiqubit system. As was stated in the main text of this work, we compute these averages by generating a random sample of 10^4 initial pure sates. These states are generated according to the Haar measure (see Ref. 38 and references therein). The Haar measure determines a uniform distribution in the space of $2^n \times 2^n$ unitary matrices which, in turn, induces a natural uniform distribution on the Hilbert 2^n-dimensional space corresponding to the n-qubit system. To generate uniformly distributed random initial states $|\Psi\rangle$ we generate random $2^n \times 2^n$ unitary matrices $U^{(n)}$ uniformly distributed according to the Haar measure, and then compute $|\Psi\rangle = U^{(n)}|\Psi_0\rangle$, where $|\Psi_0\rangle$ is a fixed n-qubit state.

To ensure that we have an appropriate sample, we consider increasing values of its size until the computed averages do not change any more (within a certain range of numerical error) with further increases of the sample size. The behavior of the numerically determined average negativity $\langle N\rangle$ as a function of the sample size, corresponding to the case of 4 qubits and $\gamma_0 t = 40$, is depicted as an illustration in Fig. 8. The behavior of $\langle N\rangle$ against the sample size corresponding to systems of 3, 5 and 6 qubits is plotted in the inset of Fig. 8. It transpires from Fig. 8 that the changes on the numerical values of $\langle N\rangle$ corresponding to an increase of the sample size from 10^4 to 10^5 are already negligible within the scale of the figures exhibited in the main text of this paper.

References

1. M. Schlosshauer, *Rev. Mod. Phys.* **76** (2005) 1267.
2. M. A. Nielsen and I. L. Chuang, *Quantum Computation and Quantum Information* (Cambridge University Press, Cambridge, 2000).
3. H. P. Breuer and F. Petruccione, *The Theory of Open Quantum Systems* (Oxford University Press, Oxford, 2002).
4. I. Bengtsson and K. Zyczkowski, *Geometry of Quantum States: An Introduction to Quantum Entanglement* (Cambridge University Press, Cambridge, 2006).
5. G. Benenti, G. Casati and G. Strini, *Principles of Quantum Computation and Information, Vol. I: Basic Concepts* (World Scientific, Singapore, 2004).
6. G. Benenti, G. Casati and G. Strini, *Principles of Quantum Computation and Information, Vol. II: Basic Tools and Special Topics* (World Scientific, Singapore, 2007).
7. M. Tichy, F. Mintert and A. Buchleitner, *J. Phys. B: At. Mol. Opt. Phys.* **44** (2011) 192001.
8. C. Simon and J. Kempe, *Phys. Rev. A* **65** (2002) 052327.
9. A. R. R. Carvalho, F. Mintert and A. Buchleitner, *Phys. Rev. Lett.* **93** (2004) 230501.
10. W. Dür and H. J. Briegel, *Phys. Rev. Lett.* **92** (2004) 180403.
11. M. Hein, W. Dür and H. J. Briegel, *Phys. Rev. A* **71** (2005) 032350.
12. L. Aolita, R. Chaves, D. Cavalcanti, A. Acín and L. Davidovich, *Phys. Rev. Lett.* **100** (2008) 080501.
13. M. P. Almeida *et al.*, *Science* **316** (2007) 579.

14. A. Salles *et al.*, *Phys. Rev. A* **78** (2008) 022322.
15. L. Aolita *et al.*, *Phys. Rev. A* **79** (2009) 032322.
16. O. Gühne, F. Bodoky and M. Blaauboer, *Phys. Rev. A* **78** (2008) 060301.
17. F. Bodoky, O. Gühne and M. Blaauboer, *J. Phys.: Cond. Mat.* **21** (2009) 395602.
18. S. Campbell, M. S. Tame and M. Paternostro, *New J. Phys.* **11** (2009) 073039.
19. A. Borras, A. P. Majtey, A. R. Plastino, M. Casas and A. Plastino, *Phys. Rev. A* **79** (2009) 022108.
20. M. Siomau, *J. Phys. B: At. Mol. Opt. Phys.* **45** (2012) 035501.
21. K. Zyczkowski, P. Horodecki, M. Horodecki and R. Horodecki, *Phys. Rev. A* **65** (2001) 012101.
22. T. Yu and J. H. Eberly, *Phys. Rev. Lett.* **93** (2004) 140404.
23. T. Yu and J. H. Eberly, *Science* **323** (2009) 598.
24. A. Al-Qasimi and D. F. V. James, *Phys. Rev. A* **77** (2008) 012117.
25. Y. S. Weinstein, *Phys. Rev. A* **79** (2009) 012318.
26. C. E. López *et al.*, *Phys. Rev. Lett.* **101** (2008) 080503.
27. B. Bellomo, R. Lo Franco and G. Compagno, *Phys. Rev. Lett.* **99** (2007) 160502.
28. B. Bellomo, R. Lo Franco and G. Compagno, *Phys. Rev. A* **77** (2008) 032042.
29. Y.-J. Zhang, Z.-X. Man, X.-B. Zou, X.-J. Xia and G.-C. Guo, *J. Phys. B: At. Mol. Opt. Phys.* **43** (2010) 045502.
30. Z.-X. Man, Y.-J. Xia and N. Ba An, *New J. Phys.* **12** (2010) 033020.
31. A. Hamadou-Ibrahim, A. R. Plastino and A. Plastino, *Braz. J. Phys.* **39** (2009) 408.
32. A. Hamadou-Ibrahim, A. R. Plastino and C. Zander, *J. Phys. A: Math. Gen.* **43** (2010) 055305.
33. J. H. Cole, *J. Phys. A: Math. Theor.* **43** (2010) 135301.
34. J. Zhou, C. Wu, M. Zhu and H. Guo, *J. Phys. B: At. Mol. Opt. Phys.* **42** (2009) 215505.
35. L. Mazzola, S. Maniscalco, J. Piilo and K.-A. Suominen, *J. Phys. B: At. Mol. Opt. Phys.* **43** (2010) 085505.
36. Z. He, J. Zou, B. Shao and S.-Y. Kong, *J. Phys. B: At. Mol. Opt. Phys.* **43** (2010) 115503.
37. Q.-J. Tong, J.-H. An, H.-G. Luo and C. H. Oh, *J. Phys. B: At. Mol. Opt. Phys.* **43** (2010) 155501.
38. J. Batle, M. Casas, A. R. Plastino and A. Plastino, *Phys. Lett. A* **296** (2002) 251.
39. I. D. K. Brown, S. Stepney, A. Sudbery and S. L. Braunstein, *J. Phys. A: Math. Gen.* **38** (2005) 1119.
40. A. Borras, A. R. Plastino, J. Batle, C. Zander, M. Casas and A. Plastino, *J. Phys. A: Math. Gen.* **40** (2007) 13407.
41. F. Mintert and A. Buchleitner, *Phys. Rev. Lett.* **98** (2007) 140505.
42. F. Mintert, M. Kus and A. Buchleitner, *Phys. Rev. Lett.* **92** (2004) 167902.
43. A. Higuchi and A. Sudbery, *Phys. Lett. A* **273** (2000) 213.
44. A. Borras, A. P. Majtey, A. R. Plastino, M. Casas and A. Plastino, *Phys. Rev. A* **79** (2009) 022112.